Origin of β-Hairpin Stability in Solution: Structural and Thermodynamic Analysis of the Folding of a Model Peptide Supports Hydrophobic Stabilization in Water

Allister J. Maynard, Gary J. Sharman, and Mark S. Searle*

Contribution from the Department of Chemistry, University of Nottingham, University Park, Nottingham NG7 2RD, U.K.

Received August 4, 1997

Abstract: The origin of the stability of isolated β-hairpins in aqueous solution is unclear with contrasting opinions as to the relative importance of interstrand hydrogen bonding, hydrophobic interactions, and conformational preferences, the latter being associated largely with the turn sequence. We have designed an unconstrained 16-residue peptide that we show folds autonomously in water to form a β-hairpin that mimics the two-stranded anti-parallel β-sheet DNA binding motif of the *met* repressor dimer. The designed peptide, with a type I′ turn (INGK), is shown by CD and a range of NMR parameters to be appreciably folded (≈50% at 303 K) in aqueous solution with the predicted alignment of the peptide backbone. We show that the folding transition approximates to a two-state model. The hairpin has a marked temperature-dependent stability, reaching a maximum value at 303 K in water with both lower and higher temperatures destabilizing the folded structure. Van't Hoff analysis of Hα chemical shifts, reveals that folding is endothermic and entropy-driven in aqueous solution with a large negative ΔC_p, all of which are reminiscent of proteins with hydrophobic cores, pointing to the hydrophobic effect as the dominant stabilizing interaction in water. We have examined the conformational properties of the C-terminal β-strand (residues 9−16) in isolation and have shown that $^3J_{\alpha N}$ values and backbone intra- and inter-residue Hα-NH NOE intensities deviate from those predicted for a random coil, indicating that the β-strand has a natural predisposition to adopt an extended conformation in the absence of secondary structure interactions. A family of β-hairpin structures calculated from 200 (distance and torsion angle) restraints using molecular dynamics shows that the conformation of the hairpin mimics closely the DNA binding face of the *met* repressor dimer (backbone RMSD between corresponding β-strands of 1.0 ± 0.2 Å).

Introduction

A β-hairpin represents the simplest conceivable model of an anti-parallel β-sheet, consisting of two β-strands linked by a short loop. While short peptides have been widely and successfully adopted in probing the stability of α-helical[1] and β-turn[2] structures, only recently have sequences been identified that fold autonomously in water to form monomeric β-hairpins.[3−13] Given the prominent position of anti-parallel β-sheet as a major component of regular secondary structure in proteins, a β-hairpin represents a context-free model[14] for examining the nature of β-sheet stabilizing interactions relevant to protein stability and initiation events during folding.

The origin of the stability of isolated β-hairpins in aqueous solution is unclear with contrasting opinions as to the relative importance of interstrand hydrogen bonding,[9] hydrophobic interactions[7,8] and conformational preference (steric factors) largely relating to the turn sequence.[5,11] Several short peptides (≤20 residues) have now been characterized that adopt β-hairpin conformations in aqueous solution.[3−13] In a number of cases, the sequence-dependent stability has been investigated to establish such factors as the role of β-turn geometry[5,11] or interstrand side chain−side chain interactions[3,8] in structure

* Corresponding author. Fax: 0115 951 3564. E-mail: mark.searle@nottingham.ac.uk.

(1) For example, see: (a) Scholtz, J. M.; Baldwin, R. L. *Annu. Rev. Biophys. Biomol. Struct.* **1992**, *21*, 95. (b) Chakrabartty, A.; Kortemme, T.; Baldwin, R. L. *Protein Sci.* **1994**, *3*, 843. (c) O'Neil, K. T.; Degrado, W. F. *Science* **1990**, *250*, 646. For N and C-capping preferences, see: (d) Doig, A. J.; Baldwin, R. L. *Protein Sci.* **1995**, *4*, 1325.

(2) For example, see: (a) Rose, G. D.; Gierasch, L. M.; Smith, J. A. *Adv. Protein Chem.* **1985**, *37*, 1. (b) Wright, P. E.; Dyson, H. J.; Lerner, R. A. *Biochemistry* **l988**, *27*, 7167. (c) Liang, G. B.; Rito, C. J.; Gellman, S. H. *J. Am. Chem. Soc.* **1992**, *114*, 4440.

(3) Blanco, F. J.; Jimenez, M. A.; Herranz, J.; Rico, M.; Santoro, J.; Nieto, J. L. *J. Am. Chem. Soc.* **1993**, *115*, 5887.

(4) DeAlba, E.; Blanco, F. J.; Jimenez, M. A.; Rico, M.; Nieto, J. L. *Eur. J. Biochem.* **1995**, *233*, 283.

(5) De Alba, E.; Jimenez, M. A.; Rico, M. *J. Am. Chem. Soc.* **1997**, *119*, 175.

(6) Blanco, F. J.; Rivas, G.; Serrano, L. *Nat. Struct. Biol.* **1994**, *1*, 584.

(7) Searle, M. S.; Williams, D. H.; Packman, L. C. *Nat. Struct. Biol.* **1995**, *2*, 999.

(8) Ramirez-Alvarado, M.; Blanco, F. J.; Serrano, L. *Nat. Struct. Biol.* **1996**, *3*, 604.

(9) Constantine, K. L.; Mueller, L.; Andersen, N. H.; Tong, H.; Wandler, C. F.; Friedrichs, M. S.; Bruccoleri, R. E. *J. Am. Chem. Soc.* **1995**, *117*, 10841.

(10) Friedrichs, M. S.; Stouch, T. R.; Bruccoleri, R. E.; Mueller, L.; Constantine, K. L. *J. Am. Chem. Soc.* **1995**, *117*, 10855.

(11) Haque, T. S.; Gellman, S. H. *J. Am. Chem. Soc.* **1997**, *119*, 2303.

(12) DeAlba, E.; Jimenez, M. A.; Rico, M.; Nieto, J. L. *Folding Des.* **1996**, *1*, 133.

(13) Maynard, A. J.; Searle, M. S. *J. Chem. Soc., Chem. Commun.* **1997**, 1297.

(14) Energetic contributions to protein stability of residues in β-sheets have been examined by protein engineering experiments and the context-dependence investigated: (a) Minor, D. L.; Kim, P. S. *Nature* **1994**, *367*, 660. (b) Minor, D. L.; Kim, P. S. *Nature* **1994**, *371*, 264. (c) Smith, C. K.; Withka, J. M.; Regan, L. *Biochemistry* **1994**, *33*, 5510.

S0002-7863(97)02676-0 CCC: $15.00
Published on Web 02/24/1998

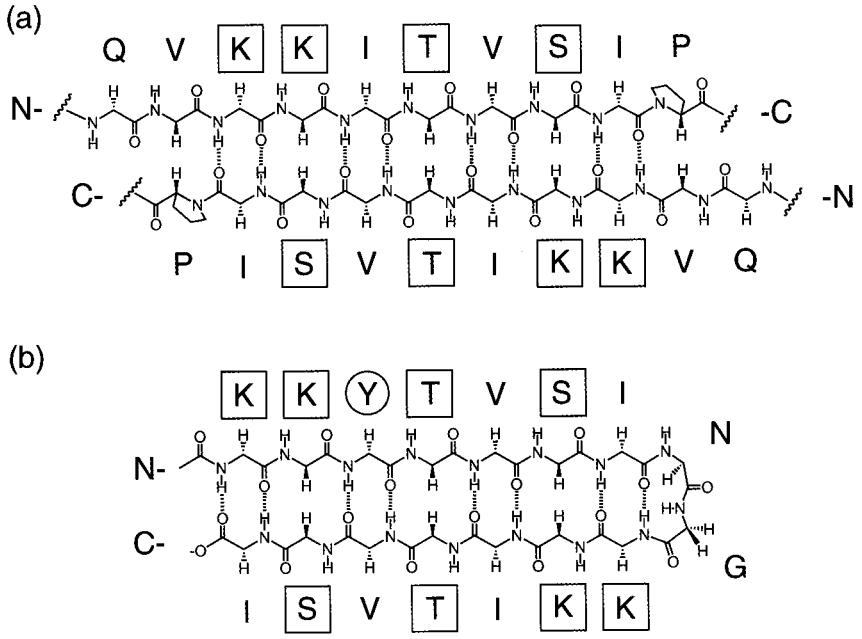

Figure 1. (a) Anti-parallel alignment of the two β-strands of the DNA recognition motif of the *met* repressor protein dimer. Key residues for DNA binding and recognition are highlighted in square boxes. (b) Designed 16-residue β-hairpin analogue of (a). Ile at position 3 in the native sequence was changed to Tyr to improve NMR "visibility". The sequence is numbered as follows: N-Ac-$K^1K^2Y^3T^4V^5S^6I^7N^8G^9K^{10}K^{11}I^{12}T^{13}V^{14}S^{15}I^{16}$.

stabilization. An analysis by Haque and Gellman[11] of the conformation of a family of peptides derived from the N-terminus of ubiquitin has established that for two-residue Pro-X turns the geometry associated with the type I′ or II′ conformation (^{D}Pro-X) promotes folding, but type I and II turns (^{L}Pro-X), which are seldom associated with two-residue turns in proteins,[15] destabilize the β-hairpin. These observations explain earlier results where insertion of a two-residue ^{L}Pro-X turn resulted in the formation of a three-residue (bulged) turn[7,12] and subsequent non-native strand alignment.[7] On the basis of this data, these authors argue that "conformational proclivity" of the peptide backbone (a combination of torsional preferences, steric repulsions disfavoring alternative folding arrangements, and entropic factors) plays a significant role in hairpin stabilization that is equally as important as hydrogen-bonding and hydrophobic interactions.[11] Similarly, de Alba et al.[5] have demonstrated the important role of the turn sequence in dictating the register of hydrogen-bonding interactions in the flanking strand sequences.

Alternatively, Ramirez-Alvarado et al.[8] have established, from studies of three structural variants involving substitution with Ala, that hydrophobic side chain−side chain interactions are important to the stability of a designed 12-residue hairpin. A similar conclusion was reached, also from studies of a peptide derived from the N-terminal sequence of ubiquitin,[7] on the basis of the many NOEs that were observed between nonpolar side chains in the folded hairpin. In contrast, others have proposed that transient interstrand hydrogen bonding provides the major stabilizing interaction in aqueous solution[9] because small peptides were considered unable to bury a large enough fraction of their hydrophobic surface area to promote folding.

To address the issue of the origin of β-hairpin stability in solution, we present an analysis of the structure and thermodynamic stability of a designed β-hairpin (Figure 1), that we have recently shown by CD and NMR to fold to a significant degree (≈50%) in water,[13] with further stabilization apparent in aqueous methanol solution. The Hα chemical shift has been used widely as an excellent probe of protein secondary structure.[16] An analysis of the temperature dependence of these shifts for the β-hairpin in a number of solvent systems has enabled us to determine in detail its thermodynamic profile. The unusual temperature-dependent stability of the hairpin in water is reminiscent of proteins with hydrophobic cores,[17] establishing the hydrophobic effect as the dominant structure stabilizing interaction in water.

Materials and Methods

Synthesis and Purification of Peptides. Peptides were synthesized using standard Fmoc solid-phase chemistry.[18,19] At the eight residue stage of synthesis, half of the resin was removed, acetylated, and cleaved, while the remainder was carried through to give the 16-residue peptide. Both peptides were then purified by reverse phase HPLC on a C8 column (Applied Biosystems Aquapore, 10 mm × 100 mm). A flow rate of 8 mL min^{-1} was used, with isocratic buffer A 95%/buffer B 5% for 5 min, followed by a linear gradient of 5 to 100% buffer B over 30 min (buffer A: water, 0.1% trifluoroacetic acid; buffer B: 30% water, 70% acetonitrile, 0.1% trifluoroacetic acid). The main fractions from successive runs were combined, evaporated under reduced pressure, redissolved in water, and lyophilized to give a white, fluffy powder. Sample purity was checked by analytical HPLC, plasma desorption mass spectrometry, and ^{1}H NMR spectroscopy.

Peptide Aggregation. NMR chemical shifts and line widths were shown to be independent of peptide concentration in the range 8 mM to 30 μM,[13] which, together with correlation times implied by temperature-dependent NOE intensities, strongly suggests that the peptide remains monomeric in solution at the concentration used for 2D NMR analysis (2−4 mM).

CD Studies. CD spectra were acquired using an AVIV model 62DS spectrometer (Aviv associates), using a 1-cm path length cell. Stock peptide solutions were prepared by weighing sufficient peptide to give

(15) Sibanda, B. L.; Thornton, J. M. *J. Mol. Biol.* **1993**, *229*, 428.

(16) (a) Wishart, D. S.; Sykes, B. D.; Richards, F. M. *J. Mol. Biol.* **1991**, *222*, 311. (b) Wishart, D. S.; Sykes, B. D.; Richards, F. M. *Biochemistry* **1992**, *31*, 1647.

(17) (a) Baldwin, R. L. *Proc. Natl. Acad. Sci. U.S.A.* **1986**, *83*, 8069. (b) Murphy, K. P.; Privalov, P. L.; Gill, S. J. *Science* **1990**, *247*, 559. (c) Murphy, K. P.; Gill, S. J. *J. Mol. Biol.* **1991**, *222*, 699.

(18) Bodanszky, M.; Bodanszky, A. *The Practice of Peptide Synthesis;* 2nd ed.; Springer-Verlag: Berlin, 1994.

(19) Atherton, E.; Sheppard, R. C. In *Solid Phase Peptide Synthesis-Practical Approach;* Atherton, E., Ed.; IRL Press: Oxford, U.K., 1989.

1 mL of 1 mM solution, and the pH was adjusted to 3.9. Samples were prepared by diluting the stock solution with water or aqueous methanol to give 7.5 μM solutions for analysis by CD. Typically nine scans were acquired over the wavelength range 190−250 nm in 0.2 nm steps using a band width of 1 nm at 298 K. The resulting data were smoothed and baseline-corrected.

NMR Studies. All NMR experiments were performed on a Brüker DRX500 spectrometer. Phase-sensitive DQF-COSY,[20] TOCSY,[21] NOESY,[22] and ROESY[23,24] experiments were performed by collecting 1−2K points in $f2$ and 400−600 points in $f1$. Quadrature detection in $f1$ was achieved using TPPI, and solvent suppression was achieved by presaturation. TOCSY experiments employed a spin locking field of 5 kHz, and ROESY experiments, 2 kHz. Mixing times of 100 and 200 ms were used in NOESY experiments. Data were processed on a Silicon Graphics Indy workstation using Brüker XWINNMR software. Typically, a sine-squared window function shifted by $\pi/4-\pi/2$ was applied in both dimensions, with zero filling in $f1$ to 1K points. For the measurement of coupling constants, high-resolution DQF-COSY and z-filtered TOCSY with 8K points in $f2$ were used. Data were strip-transformed with zero filling to 32K in $f2$ with a Gaussian window function applied. Coupling constants were measured by deconvolution of extracted rows using a Gaussian line-fitting routine. One-dimensional spectra were acquired with 32K data points and processed with 1−2 Hz line-broadening or using a Gaussian window function for resolution enhancement.

To examine the effects of temperature and solvent composition on Hα chemical shifts an unstructured 20-amino acid peptide fragment derived from the N-terminus of the B1 domain of protein L was used as a reference compound: sequence VTIKANLITPSGTQTAEFKG. The calculated RMS Hα chemical shift deviation from the random coil values of Wüthrich[25] excluded T9 (underlined), which has an anomalous shift due to the neighboring proline.

Thermodynamic Analysis. We have assumed a two-state model for folding as discussed in detail in the text. The equilibrium constant for folding (K) is given by

$$K = \upsilon/(1 - \upsilon) \tag{1}$$

where υ is the fraction of folded peptide, which is related to the experimentally determined chemical shift deviation from random coil value $\Delta\delta_{H\alpha}$. Similar plots of $\Delta\delta_{H\alpha}$ versus T were observed for all residues, and the RMS$\Delta\delta_{H\alpha}$ value was used rather than an average; this also took into account the different sign of $\Delta\delta_{H\alpha}$ for residues in the turn, hence

$$\upsilon = \mathrm{RMS}\Delta\delta_{H\alpha}/\mathrm{RMS}\Delta\delta_{\mathrm{limit}} \tag{2}$$

where RMS$\Delta\delta_{\mathrm{limit}}$ is the limiting shift for the fully folded hairpin. Random coil chemical shift values used were those of Wüthrich.[25] Using standard thermodynamic equations[26]

$$\Delta G^\circ = \Delta H^\circ - T\Delta S^\circ \tag{3}$$

$$\Delta G^\circ = -RT \ln K \tag{4}$$

substitution and rearrangement gives

$$\mathrm{RMS}\Delta\delta_{H\alpha} = \mathrm{RMS}\Delta\delta_{\mathrm{limit}}[\exp((T\Delta S^\circ - \Delta H^\circ)/RT)]/[1 + \exp((T\Delta S^\circ - \Delta H^\circ)/RT)] \tag{5}$$

Equation 5 fits the data for the temperature dependence of RMS$\Delta\delta_{H\alpha}$ values in 50% (v/v) aqueous methanol very well (see Figure 6) and suggests that ΔS° and ΔH° are independent of temperature in this solvent, in agreement with protein-folding studies and data on the solubility of hydrocarbons in mixed solvents which show ΔC_p° to be $\approx$0 under these conditions. RMS$\Delta\delta_{\mathrm{limit}}$, corresponding to the fully folded state, was determined iteratively to be 0.50 ppm. Equation 5 does not, however, fit the data at lower methanol concentrations and in pure water, where ΔH° and ΔS° appear to be temperature-dependent, implying a change in heat capacity on folding.[17] Equation 5 was modified to allow for this temperature dependence using the expressions

$$\Delta H^\circ = \Delta H^\circ_{298} + \Delta C^\circ_p(T - 298) \tag{6}$$

$$\Delta S^\circ = \Delta S^\circ_{298} + \Delta C^\circ_p \ln (T/298) \tag{7}$$

relating ΔH° and ΔS° at temperature T to ΔH°_{298} and ΔS°_{298}.[26] Hence, substituting into eq 5 gives

$$\mathrm{RMS}\Delta\delta_{H\alpha} = \mathrm{RMS}\Delta\delta_{\mathrm{limit}}[\exp(x/RT)]/[1 + \exp(x/RT)] \tag{8}$$

where $x = [T(\Delta S^\circ_{298} + \Delta C^\circ_p \ln(T/298)) - (\Delta H^\circ_{298} + \Delta C^\circ_p(T - 298))]$. Equation 8 was used to determine ΔH°_{298}, ΔS°_{298}, ΔC_p° and RMS$\Delta\delta_{\mathrm{limit}}$ iteratively from the data for RMS$\Delta\delta_{H\alpha}$ versus T in water and 20% (v/v) aqueous methanol (see Table 3). The value for RMS$\Delta\delta_{\mathrm{limit}}$ determined in this way was in excellent agreement with the value determined from the 50% methanol data at low temperature using eq 5. This value for RMS$\Delta\delta_{\mathrm{limit}}$ was used subsequently to decrease the number of iterated variables. Further, the thermodynamic parameters derived were shown to be independent of starting point by using many different initial values for ΔH°_{298}, ΔS°_{298}, ΔC_p° and RMS$\Delta\delta_{\mathrm{limit}}$, all of which converged to the same values for a particular data set. To increase confidence in the results, the value of ΔC_p° was fixed at various values (±50%) other than that determined by iteration, while ΔH°_{298}, ΔS°_{298} and RMS$\Delta\delta_{\mathrm{limit}}$ were determined iteratively. Higher and lower values for ΔC_p than determined by the iteration process produced markedly poorer fits to the data. Final error bounds were determined from the curve-fitting routine, but also by using Hα shifts for the 8-mer (corresponding to the isolated C-terminal β-strand) as a reference state rather than published random coil shifts.[25] Quoted errors reflect the range of values determined using these different methods.

Structure Calculations. Starting structures were generated using DYANA 1.2.[27] A total of 170 upper-limit distance restraints derived from NOEs were classified as strong (<2.7 Å), medium (<3.6 Å), and weak (<5 Å). In addition, 30 angle constraints, derived using HABAS from measured Hα−NH coupling constants and NOE-derived distance restraints, were also applied. A total of 30 structures were annealed using 8000 dynamics steps followed by 1000 minimization steps. Three structures were then used from this ensemble as starting structures for molecular dynamics simulations using AMBER 4.1[28] and the same set of distance and dihedral restraints. A total simulation time of 100 ps was used according to the following protocol: (i) the temperature was increased from 1 to 1200 K over the first 30 ps, (ii) temperature was held constant for 20 ps, (iii) temperature was reduced to 300 K over 20 ps, (iv) temperature held at 300 K for 10 ps, and (v) temperature was reduced to zero over 10 ps and held at constant temperature for 10 ps. Distance and dihedral restraints were introduced over the first 2 ps by ramping the restraint force constants from 0 to 32 kcal mol^{-1} Å^{-2} and 0 to 32 kcal mol^{-1} rad^{-2}. Different random seeds were employed for each run, with starting velocities being assigned from a Maxwellian distribution at 50 K. All parameters were taken from the AMBER 94 force field. The SHAKE algorithm was used allowing a step size of 2 fs. An implicit solvent model was used, employing a distance-dependent dielectric and an electrostatic cut-off

(20) Piantini, U.; Sorensen, O. W.; Ernst, R. R. *J. Am. Chem. Soc.* **1982**, *104*, 6800.
(21) Braunschweiler, L.; Ernst, R. R. *J. Magn. Reson.* **1983**, *53*, 521.
(22) Jeener, J.; Meier, B. H.; Bachmann, P.; Ernst, R. R. *J. Phys. Chem.* **1979**, *71*, 4546.
(23) Bax, A.; Davis, D. G. *J. Magn. Reson.* **1985**, *63*, 207.
(24) Bothner-by, A. A.; Stephens, R. L.; Lee, J. M.; Warren, C. D.; Jeanloz, R. W. *J. Am. Chem. Soc.* **1984**, *106*, 811.
(25) Wüthrich, K. *NMR of Proteins and Nucleic Acids*; Wiley: New York, 1986.
(26) Atkins, P. W. *Physical Chemistry*, 6th ed.; Oxford University Press: Oxford, U.K., 1998.
(27) Güntert, P.; Mumenthaler, C.; Wüthrich, K. *J. Mol. Biol.* **1997**, *273*, 283.
(28) Pearlman, D. A.; Case, D. A.; Caldwell, J. W.; Ross, W. S.; Cheatham, T. E., III; Ferguson, D. M.; Siebel, G. L.; Singh, C.; Weiner, P. K.; Kollman, P. A. *AMBER 4.1*; University of California, San Francisco, CA, 1995.

of 9 Å. The resulting structures were analyzed using MOLMOL[29] and WHATCHECK.[30]

Results and Discussion

Peptide Design: A β-Hairpin Mimic of the *met* Repressor Dimer. The β-hairpin peptide was designed, in the first instance, to mimic the two-stranded anti-parallel β-sheet DNA binding motif of the *met* repressor dimer,[31] providing a simple peptide-based template for probing protein−DNA recognition. The two anti-parallel strands of the *met* repressor formed at the interface of the dimer, together with the side chains crucial to protein−nucleic acid recognition, are illustrated in Figure 1a. Evidence that small peptides can bind to nucleic acids with high affinity and in a sequence-specific manner has recently been illustrated by work with 14−17 residue arginine-rich peptides representing the recognition domain of the bovine immunodeficiency virus transcriptional activator protein (BIV tat).[32,33] The peptide binds as a β-hairpin motif to the TAR sequence located at the 5′-end of viral mRNAs. The peptides are unstructured in solution[34] but adopt a folded conformation within the major groove of RNA. We show that our peptide analogue of the *met* repressor folds into a monomeric β-hairpin in water with an alignment of the polypeptide backbone and residue side chains such as to mimic the DNA recognition motif of the *met* repressor. Our choice of amino acid sequence was based on the necessity to incorporate the key residues in the correct spatial relationship for DNA binding to the *met* "box" [sequence d(AGACGTCT)][35] and simultaneously maximize the stability of the folded hairpin in aqueous solution by optimizing both the β-turn sequence (type I′) and by including residues that are statistically more likely to be found in a β-sheet or exert some structure-stabilizing interaction.

The two β-strands of the *met* repressor dimer align as shown in Figure 1a, with each strand carrying the KKXTXSX recognition sequence. The simplest peptide analogue capable of mimicking this anti-parallel alignment of two β-strands is a β-hairpin structure of 16 residues, where the two strands are linked by a β-turn sequence. The most abundant β-hairpins in the protein structure data base (PDB) are those with two residue turns[36] with the type I′ variety being most common.[37] Statistical analysis shows that the sequence Asn-Gly appears to be particularly favored.[38] The choice of a type I′ turn over a type I turn ensures that the hairpin has the necessary right-handed twist observed in protein β-sheets,[11,39,40] and as evident in the *met* repressor DNA recognition motif.[31] We, and others, have shown that altering the native bulged turn sequence to that of a two-residue type I turn sequence (Asn-Pro-Asp-Gly) is not compatible with this twist,[7,8,12,39,41] resulting in a bulged turn being re-established with a realignment of the two strands into a non-native conformation. Thus, our choice of sequence was based on a two-residue turn (Asn-Gly) and the alignment of key residues for DNA recognition as highlighted in Figure 1b.

It is noteworthy that a number of features of the proposed folded conformation suggest that the peptide is favorably disposed to folding on the basis of the statistical analysis of β-hairpin structures in the protein data base described by Ramirez-Alvarado et al.[8] For example, charged residues are found to be particularly abundant at position +1 (XNGX; residue 10 in this sequence), coinciding with the first requisite Lys in the C-terminal strand. Val, Ile, Ser, and Tyr have been shown to be common at position −1 (XNGX; residue 7). This position is occupied by Ile in the native sequence, suggesting that the turn sequence INGK should have a high propensity for forming a type I′ turn. Our only change to the sequence in the β-strand regions was to replace Ile (residue 3) on the non-DNA binding face with Tyr for the purpose of removing some of the sequence degeneracy, but also as an NMR probe for both ring current effects and long-range NOEs in a well-resolved region of the spectrum. In addition, several studies of proteins, β-hairpin-forming peptides and α-helices have shown that side chain interactions between Tyr or Phe and Val, Ile, or Leu can lead to structure-stabilizing interactions through burial of hydrocarbon from access to solvent.[42−44] In this case we have introduced a Tyr → Val interaction between residues in hydrogen-bonding positions on opposite strands of the hairpin. In general, β-branched amino acids are found in abundance in the native sequence, in particular, positions +4 and −4 (residues 4 and 13) are occupied by Thr, which has one of the highest intrinsic preferences for β-sheet formation.[14,45] Two threonines are often found opposite each other in non-hydrogen-bonding sites in anti-parallel β-sheets,[46] illustrating a further natural feature of the amino acid sequence that predisposes it to adopt an anti-parallel β-sheet. The presence of two KK "doublets" within the sequence should aid solubility and also significantly reduce the possibility of peptide aggregation, since hydrophilic side chains are placed on both faces of the hairpin rather than the more typical arrangement that produces one hydrophobic and one hydrophilic face.

Conformational Analysis by Circular Dichroism. The N-acetylated 16-mer shown in Figure 1b has been studied by far-UV circular dichroism (CD) spectroscopy in aqueous solution at pH 3.9 and 7.5 μM. We observe a negative ellipticity at 216 nm that suggests that the peptide forms a significant proportion of folded structure in purely aqueous solution with the absorption profile reminiscent of β-structure (both turn and sheet) in equilibrium with some random coil (negative ellipticity below 198 nm) (Figure 2).[47,48] Titration of the peptide with methanol (at constant peptide concentration) produces a deepening of the minimum at 216 nm and formation of a maximum at ≈200 nm, indicative of a displacement of the equilibrium already present in aqueous solution further toward the folded state. The structural transition is effectively complete at 50% (v/v) methanol, with an isodichroic point at 209 nm in the methanol titration, suggesting a two-state folding transition between random coil and β-structure. We have used the

(29) Koradi, R.; Billeter, M.; Wüthrich, K. *J. Mol. Graphics* **1996**, *14*, 51.
(30) Hooft, R. W. W.; Vriend, G.; Sander, C.; Abola, E. E. *Nature* **1996**, *381*, 272.
(31) Somers, W. S.; Phillips, S. E. V. *Nature* **1992**, *359*, 387.
(32) Puglisi, J. D.; Chen, L.; Blanchard, S.; Frankel, A. D. *Science* **1995**, *270*, 1200.
(33) Ye, X. M.; Kumar, R. A.; Patel, D. J. *Chem. Biol*. **1995**, *2*, 827.
(34) Chen, L.; Frankel, A. D. *Proc. Natl. Acad. Sci. U.S.A.* **1995**, *92*, 5077.
(35) (a) Rafferty, J. B.; Somers, W. S.; Saint Girons, I.; Phillips, S. E. V. *Nature* **1989**, *341*, 705. (b) Phillips, S. E. V. *Curr. Opin. Struct. Biol.* **1991**, *1*, 89.
(36) Sibanda, B. L.; Thornton, J. M. *J. Mol. Biol.* **1993**, *229*, 428.
(37) Hutchinson, E. G.; Thornton, J. M. *Protein Sci.* **1994**, *3*, 2207.
(38) Sibanda, B. L.; Thornton, J. M. *Methods Enzymol.* **1991**, *202*, 59.
(39) Chothia, C. *J. Mol. Biol.* **1973**, *75*, 295.
(40) Richardson, J. S. *Adv. Protein Chem.* **1981**, *34*, 167.
(41) Chou, K. C.; Nemethy, G.; Scheraga, H. A. *J. Mol. Biol.* **1983**, *168*, 389.
(42) Smith, C. K.; Regan, L. *Science* **1995**, *270*, 980.
(43) Padmanabhan, S.; Baldwin, R. L. *J. Mol. Biol.* **1994**, *241*, 706.
(44) Kemmink, J.; Creighton, T. E. *J. Mol. Biol.* **1993**, *234*, 861.
(45) Kim, C. W. A.; Berg, J. M. *Nature* **1993**, *362*, 267.
(46) Wouters, M. A.; Curmi, P. M. G. *Proteins Struct., Funct. Genet.* **1995**, *22*, 119.
(47) Johnson, W. C. *Annu. Rev. Biophys. Biophys. Chem.* **1988**, *17*, 145.
(48) Yang, J. T.; Wu, C. S. C.; Martinez, H. M. *Methods Enzymol.* **1986**, *130*, 208.

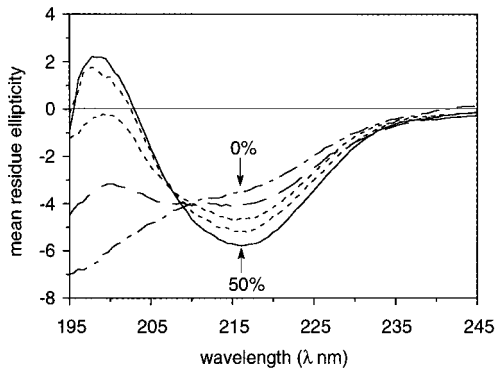

Figure 2. Far-UV circular dichroism (CD) spectra of the 16-mer in aqueous solution at 7.5 μM concentration, 298 K, and pH 3.9. Mean residue ellipticity (θ, deg cm^2 dmol^{-1} $\times$ 10^{-3}) is plotted against wavelength (λ, nm). The spectrum of the peptide in pure water is labeled 0% (reflecting the methanol concentration). The ellipticity at 216 nm becomes more negative as the methanol concentration is increased to 10, 20, 30, and 50% (v/v) at a constant peptide concentration. An isodichroic point at 209 nm suggests a two-state folding transition.

ellipticity at 216 nm to estimate the population of β-hairpin present in solution by considering the negative ellipticity value at 50% (v/v) methanol as one reference point for the fully folded structure, while an ellipticity of close to zero at this wavelength has been shown for a fully random coil conformation,[6,48] providing the second reference point. On this basis, the population of β-sheet in water was estimated to be ≈55%. Addition of 20% methanol to the peptide solution appears to increase the population of folded structure to ≈80%.

Structural Analysis of the β-Hairpin by ^{1}H NMR. (i) Evidence for Interstrand Interactions through Long-Range NOEs. ^{1}H NMR spectra recorded in a variety of solvents have been fully assigned using a combination of DQF-COSY, TOCSY, NOESY, and ROESY 2D data sets. ^{1}H chemical shift assignments at 278 K in water, 20% (v/v) and 50% (v/v) aqueous methanol are presented in Table 1. The most conclusive evidence for folded structure is the observation of long-range NOEs between residues in the anti-parallel strands of the β-hairpin. Several intense interstrand Hα−Hα interactions are readily detected between non-hydrogen-bonded residues (Lys2-Ser15, Thr4-Thr13, and Ser6-Lys11)[13] representing interstrand interactions along the full length of the hairpin. The pattern of NOEs is fully consistent with the anti-parallel alignment of the peptide chain shown in Figure 1b. These conclusions are confirmed by studies of the 16-mer in 90% H_2O solution where a number of cross-strand NH−NH interactions between hydrogen-bonded residues (Lys1-Ile16, Val5-Ile12 and Ile7-Lys10) are also detected (Figure 3a). The first of these interactions (Lys1-Ile16) illustrates that even the two terminal residues persist in close proximity.

The intensities of the cross-strand Hα−Hα NOEs have been used to estimate the population of folded hairpin in the different solvent systems. Full analysis over a wide range of temperatures is complicated by the position of the solvent signal and the close proximity of Hα−Hα NOEs to the diagonal. The S6−K11 NOE is resolved under most conditions and has been calibrated from ROESY data sets using the G9 Hα−Hα NOE as a fixed reference distance. The ratio of intensities was calculated to be 0.19 using the interstrand Hα−Hα separation of 2.32 Å found in regular anti-parallel β-sheets in proteins.[6,7,26] This ratio of intensities represents the limiting value corresponding to 100% folded hairpin. From the experimental ratio of intensities, we have calculated the percentage folded hairpin in water, 20% and 50% methanol at 298 K for comparison with the results from the CD analysis at a similar temperature. We estimate the populations as 44 ± 3%, 74 ± 4%, and 81 ± 6%, respectively. The errors reflect averaging of cross-peak intensities measured on both sides of the diagonal. These values are in good agreement with those estimated by CD at a similar temperature and by subsequent fitting of the temperature dependence of chemical shift data as described below (see Table 2).

(ii) Quantitative Estimate of NOE Intensities: Comparison with the Random Coil Model. We have examined local NOE interactions along the peptide chain in the context of the random coil model recently proposed on the basis of a statistical analysis of the ψ,ϕ distributions found in the protein data base.[49−52] The analysis reveals that residues in the coil regions of proteins (i.e., irregular regions of structure that are not α-helical or β-sheet) have very non-uniform ψ,ϕ populations with conformations also concentrated in the α and β regions of ψ,ϕ space.[49] More importantly, the populations are residue-specific, reflecting side chain steric interactions, hydrophobic contacts, and electrostatic interactions. Using these residue-specific ψ,ϕ distributions, NMR parameters that probe the conformational properties of each individual residue have been predicted and have been found to agree with experimental data for a number of short peptides and denatured proteins.[52,53] Perhaps the most useful aspect of the random coil model is its ability to predict the intensities of short-range and medium-range NOEs expected from the population-weighted ψ,ϕ distribution.[50,52] All sequential Hα−NH and NH−NH NOEs are predicted to be observed for a random coil conformation, reflecting the significant population of both α and β conformers for each residue in the random coil. The ratio of intensities αN(i,i+1)/NN(i,i+1) is shown to have an average value of ≈1.4, although the ratio is dependent on the residue-specific ψ,ϕ population, varying between 1.0 (Asn) and 2.7 (Ile).[52] This ratio is proposed to be significantly different when residues adopt predominantly β-strand conformation increasing to ≈55 for the regular β-sheet secondary structure found in proteins. However, the medium-range NOEs such as αN(i,i+2) and αN(i,i+3), that are evident in the random coil model as a consequence of populations of $\beta(i)\alpha(i+1)$ and $\alpha(i)\alpha(i+1)$ conformers, are not predicted to be detected for the exclusively $\beta(i)\beta(i+1)$ conformation of an extended β-strand.

We have carried out a quantitative examination of NOE intensities for the β-hairpin using NOESY data collected at 278 K at mixing times of 100 and 200 ms. The αN(i,i+1)/NN(i,i+1) NOE intensity ratio was difficult to determine experimentally for all residues because NN(i,i+1) NOEs were generally only observed for residues close to the turn (residues 7−11) being particularly strong for Asn8 and Gly9. In the β-strand regions αN(i,i+1) NOEs are very strong. Excluding the terminal residues Lys1 and Ile16, and the turn residues Asn8 and Gly9, we estimate an intensity ratio for αN(i,i+1)/NN(i,i+1) of at least 15 using both NOESY data sets, which is clearly consistent with a predominantly extended β-strand conformation rather than random coil for the sequences 2−7 and 10−15.

The NOE intensity ratio αN(i,i+1)/αN(i,i) provides a further

(49) Swindells, M. B.; MacArthur, M. W.; Thornton, J. M. *Nat. Struct. Biol.* **1995**, *2*, 596.
(50) Smith, L. J.; Fiebig, K. M.; Schwalbe, H.; Dobson, C. M. *Folding Des.* **1996**, *1*, R95.
(51) Smith, L. J.; Bolin, K. A.; Schwalbe, H.; MacArthur, M. W.; Thornton, J. M.; Dobson, C. M. *J. Mol. Biol.* **1996**, *255*, 494.
(52) Fiebig, K. M.; Schwalbe, H.; Buck, M.; Smith, L. J.; Dobson, C. M. *J. Phys. Chem.* **1996**, *100*, 2661.
(53) Bolin, K. A.; Pitkeathly, M.; Miranker, A.; Smith, L. J.; Dobson, C. M. *J. Mol. Biol.* **1996**, *261*, 443.

Table 1. ^{1}H Chemical Shift Assignments for β-Hairpin Peptide at 278 K in (a) Water, (b) 20% Aqueous Methanol and (c) 50% Aqueous Methanol Referenced to Internal (Trimethylsilyl)propionate

residue	NH	αH	βH	other		residue	NH	αH	βH	other	
(a) Chemical Shifts in Water, 278 K											
K1	8.46	4.22	1.68, 1.68	γCH$_2$	1.40, 1.33	K10	8.04	4.40	1.81, 1.77	γCH$_2$	1.43, 1.37
				δCH$_2$	1.63, 1.63					δCH$_2$	1.67, 1.67
				εCH$_2$	2.94, 2.94					εCH$_2$	2.98, 2.98
				εNH$_3^+$	7.66					εNH$_3^+$	7.66
K2	8.44	4.51	1.71, 1.71	γCH$_2$	1.44, 1.31	K11	8.58	4.51	1.71, 1.71	γCH$_2$	1.44, 1.31
				δCH$_2$	1.60, 1.60					δCH$_2$	1.60, 1.60
				εCH$_2$	2.90, 2.90					εCH$_2$	2.90, 2.90
				εNH$_3^+$	7.66					εNH$_3^+$	7.66
Y3	8.59	4.80	3.03, 2.90	δH	7.07	I12	8.79	4.35	1.86	γCH$_2$	1.45, 1.19
				εH	6.77					γCH$_3$	0.88
T4	8.48	4.61	4.04	γCH$_3$	1.14					δCH$_3$	0.82
V5	8.60	4.32	2.04	γCH$_3$	0.94, 0.94	T13	8.62	4.57	4.07	γCH$_3$	1.16
S6	8.67	4.75	3.80, 3.80			V14	8.65	4.25	1.99	γCH$_3$	0.92, 0.92
I7	8.70	4.23	1.85	γCH$_2$	1.44, 1.17	S15	8.60	4.67	3.84, 3.78		
				γCH$_3$	0.88	I16	8.08	4.13	1.86	γCH$_2$	1.41, 1.19
				δCH$_3$	0.85					γCH$_3$	0.89
N8	8.90	4.64	2.95, 2.78	γNH$_2$	7.05, 7.76					δCH$_3$	0.80
G9	8.52	4.01, 3.77									
(b) Chemical Shifts in 20% (v/v) Methanol, 278 K											
K1	8.47	4.29	1.72, 1.72	γCH$_2$	1.44, 1.35	K10	7.93	4.48	1.81, 1.81	γCH$_2$	1.44, 1.36
				δCH$_2$	1.68, 1.68					δCH$_2$	1.68, 1 68
				εCH$_2$	2.95, 2.95					εCH$_2$	2.99, 2.99
				εNH$_3^+$	7.68					εNH$_3^+$	7.68
K2	8.34	4.82	1.66, 1.66	γCH$_2$	1.39, 1.32	K11	8.54	4.72	1.73, 1.62	γCH$_2$	1.45, 1.27
				δCH$_2$	1.60, 1.60					δCH$_2$	1.57, 1.57
				εCH$_2$	2.91, 2.91					εCH$_2$	2.87, 2.87
				εNH$_3^+$	7.68					εNH$_3^+$	7.68
Y3	8.67	4.87	3.00, 2.86	δH	7.03	I12	8.93	4.45	1.83	γCH$_2$	1.41, 1.18
				εH	6.72					γCH$_3$	0.86
T4	8.55	4.95	3.96	γCH$_3$	1.12					δCH$_3$	0.82
V5	8.73	4.50	2.06	γCH$_3$	0.92, 0.92	T13	8.59	4.81	3.98	γCH$_3$	1.14
S6	8.61	5.02	3.75, 3.71			V14	8.80	4.36	1.88	γCH$_3$	0.89, 0.81
I7	8.78	4.27	1.79	γCH$_2$	1.46, 1.14	S15	8.50	4.89	3.81, 3.72		
				γCH$_3$	0.86	I16	8.23	4.16	1.87	γCH$_2$	1.43, 1.12
				δCH$_3$	0.83					γCH$_3$	0.89
N8	9.07	4.51	3.01, 2.77	γNH$_2$	7.04, 7.74					δCH$_3$	0.83
G9	8.52	3.60, 4.10									
(c) Chemical Shifts in 50% (v/v) Methanol, 278 K											
K1	8.50	4.35	1.75, 1.70	γCH$_2$	1.45, 1.36	K10	7.90	4.54	1.84, 1.84	γCH$_2$	1.45, 1.39
				δCH$_2$	1.74, 1.74					δCH$_2$	1.69, 1.69
				εCH$_2$	2.95, 2.95					εCH$_2$	3.00, 3.00
				εNH$_3^+$	7.70					εNH$_3^+$	7.76
K2	8.19	5.09	1.63, 1.57	γCH$_2$	1.38, 1.31	K11	8.50	4.87	1.74, 1.57	γCH$_2$	1.44, 1.26
				δCH$_2$	1.69, 1.69					δCH$_2$	1.57, 1.57
				εCH$_2$	2.95, 2.95					εCH$_2$	2.88, 2.88
				εNH$_3^+$	7.70					εNH$_3^+$	7.71
Y3	8.83	4.84	2.95, 2.81	δH	6.98	I12	9.02	4.50	1.81	γCH$_2$	1.41, 1.16
				εH	6.68					γCH$_3$	0.86
T4	8.58	5.17	3.88	γCH$_3$	1.10					δCH$_3$	0.82
V5	8.93	4.58	2.07	γCH$_3$	0.93, 0.89	T13	8.57	5.01	3.90	γCH$_3$	1.12
S6	8.51	5.21	3.73, 3.58			V14	9.04	4.45	1.85	γCH$_3$	0.88, 0.78
I7	8.90	4.32	1.76	γCH$_2$	1.46, 1.14	S15	8.39	5.12	3.77, 3.66		
				γCH$_3$	0.89	I16	8.43	4.22	1.90	γCH$_2$	1.46, 1.13
				δCH$_3$	0.84					γCH$_3$	0.91
N8	9.34	4.41	3.06, 2.77	γNH$_2$	7.03, 7.73					δCH$_3$	0.80
G9	8.55	4.14, 3.51									

handle on the population of β-conformers present in solution. Using the same set of 85 high-resolution structures described in the earlier analysis,[51] we have estimated the average αN(*i*,*i*) NOE intensity ratio using the ψ,φ population weighting and αN(*i*,*i*+1) average intensity previously determined.[51,52] We estimate a value for the ratio αN(*i*,*i*+1)/αN(*i*,*i*) to be ≈2.3, but larger values of ≈8 are predicted for an idealized anti-parallel β-sheet. We measure from the same NOESY data sets (see Figure 3b) an average value of >5 (range 3.6−10.6) for residues in the β-strands of the hairpin (2−7 and 10−15), again consistent with a very high proportion of extended β-structure. Significant deviations from these intensity ratios are apparent for Asn8 and Gly9 that reflect the involvement of these residues in a β-turn. Here the αN(*i*,*i*+1)/αN(*i*,*i*) NOE intensity ratio falls below 1, consistent with the (left-handed) α_L population of Asn8 and Gly9 in a type I′ turn.

(iii) Deviation of $^3J_{\alpha N}$ from Random Coil Values. The deviation of $^3J_{\alpha N}$ coupling constants from the random coil values have been determined for the 16-mer in water, 20% (v/v) and 50% (v/v) methanol at 278 K. In general, values are larger than in the random coil reflecting residues in predominantly β-strand conformation, while a smaller value for Asn8 reflects

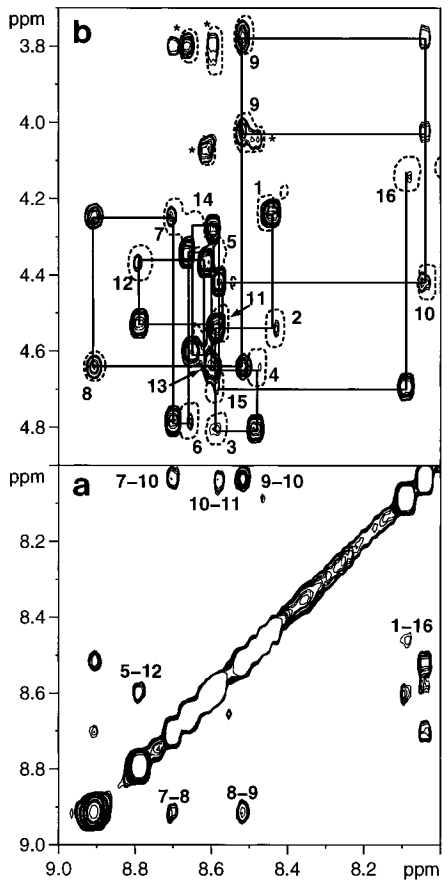

Figure 3. (a) Portion of the NOESY spectrum (200 ms mixing time) of the 16-mer at 278 K in 90% H_2O/10% D_2O solution illustrating cross-strand NH−NH NOEs that are consistent with the proposed folded structure. (b) Finger-print regions (NH to Hα) of NOESY (200 ms) and TOCSY spectra (overlayed) of the hairpin in water at 278 K. TOCSY data are plotted as a single broken contour. In general, αN(*i*,*i*) intraresidue NOEs (occuring at the same positions as TOCSY cross-peaks) are very weak for residues in extended β-strands (residues 1−7 and 10−16), while αN(*i*,*i*+1) sequential interresidue NOEs are much more intense. However, the αN(*i*,*i*) and αN(*i*,*i*+1) NOEs are of comparable intensity for N8 and G9, reflecting their positions in the β-turn. Asterisks mark the position of NH to Hβ cross-peaks in both NOESY and TOCSY. TOCSY NH to Hα cross-peaks are numbered according to the sequence N-Ac-$K^1K^2Y^3T^4V^5S^6I^7N^8G^9K^{10}K^{11}I^{12}$-$T^{13}V^{14}S^{15}I^{16}$.

Table 2. Estimates of the Population (%) of Folded β-Hairpin From (i) CD Analysis of Ellipticity at 216 nm, (ii) Interstrand Hα−Hα NOE Intensities, and (iii) Iterative Fitting of RMSΔ$\delta_{H\alpha}$ Values versus Temperature

	water	20% (v/v) aqueous methanol	50% (v/v) aqueous methanol
ellipticity at 216 nm (298 K)	55	80	>90
Hα−Hα NOE intensity (298 K)	41−47	70−78	75−86
RMSΔ$\delta_{H\alpha}$ (298 K)	47	66	86

its position in the β-turn sequence. For a number of residues $^3J_{\alpha N}$ values deviate significantly ($\Delta J_{\alpha N}$ > 1 Hz) from the expected range of random coil values[51,52] (see Figure 4). From the data collected from the peptide in water, it is noticeable that, of the residues in the N-terminal β-strand, Lys 2 and Ser 5 have the largest $\Delta J_{\alpha N}$ values as predicted by the random coil model since these residues have ϕ,ψ populations weighted toward the helical conformation. The addition of methanol generally increases the size of the deviation from random coil

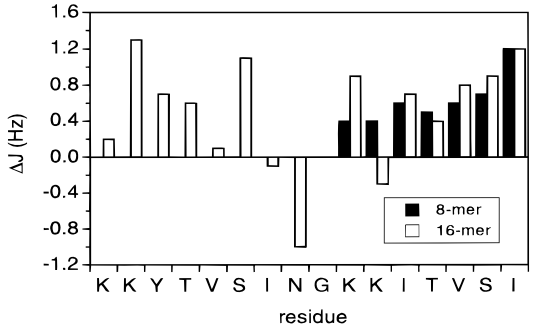

Figure 4. Calculated difference (Δ*J*) between experimental $^3J_{\alpha N}$ values and random coil values[51] for the β-hairpin and for the isolated C-terminal eight-residue fragment (residues 9−16) in water at 278 K, pH 3.9. Positive Δ*J* values reflect a higher proportion of β-conformers than found in the random coil.

values, reflecting the effects of the solvent in promoting β-hairpin formation through the stabilization of interstrand hydrogen-bonding interactions and hence restricting the conformational freedom about ϕ and ψ.

(iv) Perturbations to Hα Chemical Shifts. Analysis of the Hα chemical shifts of the peptide in water at 278 K, pH 4.0 (Figure 5a), reveals, in general, quite significant deviations from the random coil values ($\Delta\delta_{H\alpha}$) derived from studies of model tetrapeptides.[25] Using the criteria of Wishart et al.,[16] the observation of more than three contiguous residues with $\Delta\delta_{H\alpha}$ values greater than the chemical shift index value of 0.1 ppm is indicative of residues in an extended β-sheet conformation. Substantial upfield shifts are observed for the Asn and Gly residues at the center of the sequence indicative of a β-turn conformation. The plot of chemical shift deviations from random coil values has the characteristic appearance of a β-hairpin, with two extended β-strands separated at the center of the sequence by a turn region.[16,54]

The data in Figure 5a also illustrate the effects on $\Delta\delta_{H\alpha}$ values of increasing concentrations of methanol [20% (v/v) and 50% (v/v) at 278 K], reflecting the change in the position of the equilibrium between folded and unfolded states, as has been reported for a number of other model β-hairpin peptides.[55−57] $\Delta\delta_{H\alpha}$ values increase markedly upon addition of methanol, indicative of a much larger proportion of the folded conformation, as also evident from CD and NOE intensity measurements. To eliminate the possibility that the change in solvent composition alone has a significant effect on chemical shifts, we have examined an unrelated peptide of 20 residues of mixed sequence that by both CD and NMR shows no evidence for the formation of folded structure under the same solvent conditions described here (unpublished results). We have calculated an RMS difference [$\delta_{(50\%\ methanol)} - \delta_{(water)}$] of 0.02 (±0.03) ppm from the measured shifts of the peptide in the two solvents and an RMSD from reported random coil values of 0.03 (±0.04) ppm, indicating that solvation effects on chemical shifts are quite small. To test this assumption further, we have synthesized an eight-residue peptide corresponding to the C-terminal β-strand of the hairpin (residues 9−16). As for the 20-mer, the chemical shifts of the Hα protons of the 8-mer are close to random coil values (0.01 ± 0.05 ppm) over the range of temperature and

(54) Williamson, M. P.; Asakura, T.; Nakamura, E.; Demura, M. *J. Biomol. NMR* **1992**, *2*, 83.
(55) Blanco, F. J.; Jimenez, M. A.; Pineda, A.; Rico, M.; Santoro, J.; Nieto, J. L. *Biochemistry* **1994**, *33*, 6004.
(56) Cox, J. P. L.; Evans, P. A.; Packman, L. C.; Williams, D. H.; Woolfson, D. N. *J. Mol. Biol.* **1993**, *234*, 483.
(57) Searle, M. S.; Zerella, R.; Williams, D. H.; Packman, L. C. *Protein Eng.* **1996**, *9*, 559.

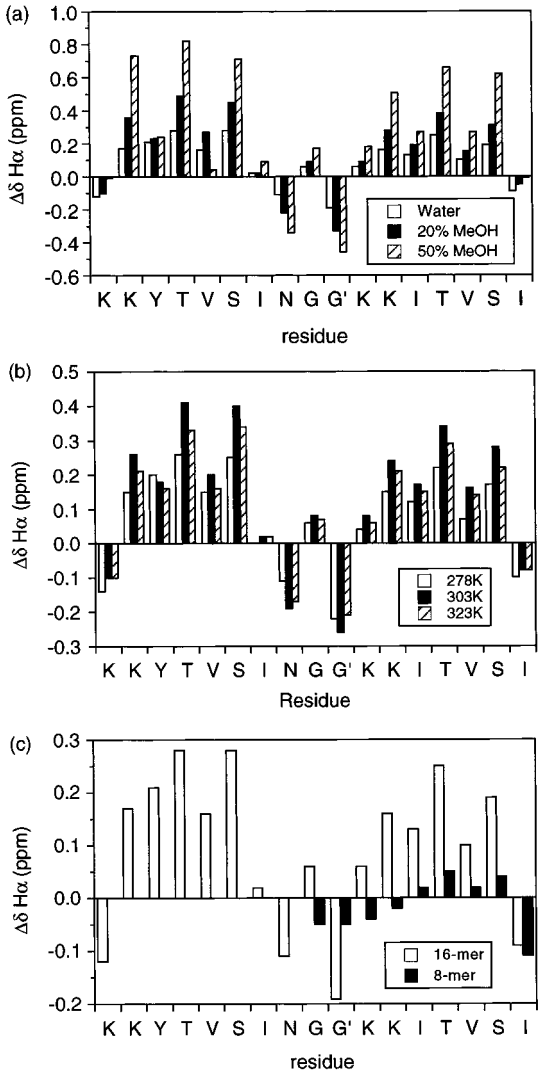

Figure 5. Plots of difference between Hα chemical shift values in the random coil and values determined experimentally ($\Delta\delta_{H\alpha}$) for (a) β-hairpin at 278 K in water, pH 3.9, in 20% (v/v) aqueous methanol, and in 50% (v/v) aqueous methanol; (b) β-hairpin in water pH 3.9 at 278, 303, and 323 K; and (c) β-hairpin and isolated C-terminal 8-mer (residues 9−16) at 278 K in water, pH 3.9.

solvent composition described in this study. The observation of such small deviations from random coil values from studies of both of these peptides under a variety of conditions suggests that only small errors are accrued in using published random coil values uncorrected for solvent effects.

Temperature Dependence of β-Hairpin Stability. In water, the hairpin has a maximum stability at 303 K, corresponding to the temperature at which the largest deviations from random coil chemical shifts are observed (Figure 5b). At higher and lower temperatures, smaller $\Delta\delta_{H\alpha}$ values are measured, reflecting a decrease in the amount of folded structure present in solution. The data show that the hairpin exhibits the unusual temperature-dependent stability characteristic of proteins with hydrophobic cores and as also observed for the solubility of hydrocarbons in water.[17] This phenomenon is attributed to $\Delta H°$ and $\Delta S°$ being temperature-dependent as a consequence of a decrease in heat capacity ($\Delta C_p°$) between the folded and unfolded states. Since all residues (with the exception of those in the terminal positions) show similar plots of $\Delta\delta_{H\alpha}$ versus T, we have used the RMS$\Delta\delta_{H\alpha}$ value over all residues, which takes into account the different sign of $\Delta\delta_{H\alpha}$ for residues in the turn region, to analyze the thermodynamics of folding. By interpreting the temperature-dependent change in RMS$\Delta\delta_{H\alpha}$ (Figure 6) as a measure of the change in population of folded peptide, an equation has been derived relating RMS$\Delta\delta_{H\alpha}$ to T in terms of $\Delta H°$, $\Delta S°$ and $\Delta C_p°$ at 298 K using standard thermodynamic expressions (see Materials and Methods). The parameters shown in Table 3 have been determined using an iterative nonlinear least-squares fitting routine. The curves of best fit are shown in Figure 6. For the purpose of assessing error bounds, we have fitted the data in Figure 6 using both the published random coil values and the chemical shifts of the 8-mer as the random coil reference state. Very similar results are obtained in both cases; the error bounds on the data in Table 3 reflect the results obtained via these two methods.

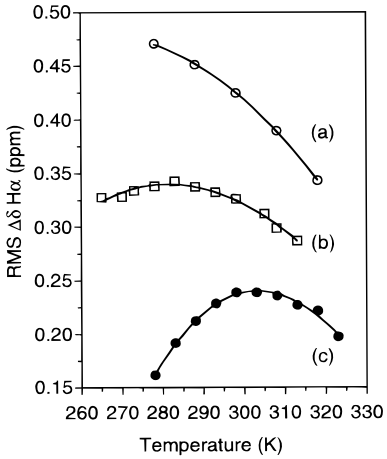

Figure 6. Plots of RMS $\Delta\delta_{H\alpha}$ values as a function of temperature for the peptide in (a) 50% (v/v) aqueous methanol, (b) 20% (v/v) aqueous methanol, and (c) water. The curves of best fit to the experimental data (correlation coefficients > 0.99 in all cases) are illustrated; thermodynamic data are presented in Table 3.

Table 3. Thermodynamic Parameters for the Folding of the β-Hairpin in Aqueous Solution, 20% (v/v) Methanol and 50% (v/v) Methanol Determined from a van't Hoff Analysis of the Temperature Dependence of Hα Chemical Shifts

solvent	$\Delta H°$ [a]	$\Delta S°$ [b]	$\Delta C_p°$ [b]
water	+7.2 (±05)	+23 (±3)	−1400 (±100)
20% (v/v) methanol	−11.7 (±0.7)	−34 (±3)	−700 (±60)
50% (v/v) methanol	−38.5 (±07)	−114 (±3)	−11 (±70)

[a] kJ mol^{-1} at 298 K. [b] J K^{-1} mol^{-1} at 298 K.

This analysis assumed that folding was a cooperative two-state process, and this assumption warrants further justification. Several lines of evidence support this assumption, including the observation of an isodichroic point at 209 nm in the CD spectrum upon titration with methanol (Figure 2), and an examination of the temperature dependence of $\Delta\delta_{H\alpha}$ values at the individual residue level. At 278 K in 50% methanol we have measured an RMS$\Delta\delta_{H\alpha}$ value over all residues of 0.48 ppm, while in water at 303 K, the RMS$\Delta\delta_{H\alpha}$ value (0.24 ppm) is one-half that in the mixed solvent (see data in Figure 5a,b). Thus, the ratio of RMS$\Delta\delta_{H\alpha}$ values under the two sets of conditions reflects the relative population of folded hairpin. When the ratio of $\Delta\delta_{H\alpha}$ values is examined at the individual residue level (Figure 7), it is readily apparent that the majority of residues reflect the same population ratio. The notable exception to this rule (excluding the terminal residues) is Ile 7. In the case of Ile 7, $\Delta\delta_{H\alpha}$ values are small (<0.1 ppm) and thus the calculated ratio is subject to large error, in contrast to many other residues which have $\Delta\delta_{H\alpha}$ values of >0.7 ppm. It appears, therefore, that the overall folded population is accurately reflected in the folded population of any individual

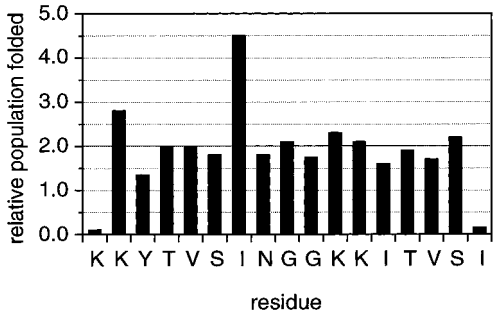

Figure 7. Relative population of folded β-hairpin estimated for each residue in 50% (v/v) aqueous methanol at 278 K versus the population in water at 303 K. Values reflect the ratio of $\Delta\delta_{H\alpha}$ values (deviation of Hα shift from random coil) under the two sets of conditions. In 50% aqueous methanol at 278 K the hairpin is >90% folded (see Table 2). A ratio close to 2 indicates that the population of folded structure in 50% aqueous methanol is twice that in water; this is reflected by the majority of residues in the hairpin.

residue, supporting our assumption of a cooperative, two-state folding pathway.

A similar test is provided by the denaturing effects of urea on the folded population in water, again using the Hα chemical shifts as a probe. The hairpin conformation proved to be highly resistant to denaturation by urea, with significant Hα chemical shift deviations still evident at a concentration of 7 M at pH 4.5, together with the same temperature-dependent stability profile described above. The ratio of RMS$\Delta\delta_{H\alpha}$ values in pure water and 7 M urea at 278 K was estimated to be 1.6. The ratio of $\Delta\delta_{H\alpha}$ values was again examined at the individual residue level (data not shown) and revealed that a ratio close to 1.6 was uniformly represented throughout the sequence, with the exception of the terminal residues. Both the temperature-dependent effects and urea concentration effects on $\Delta\delta_{H\alpha}$ values add weight to a two-state folding model.

Thermodynamic Analysis of Folding. The thermodynamic parameters for folding derived as described in the previous section are presented in Table 3. Folding in water is endothermic and entropy-driven at 298 K with an associated negative $\Delta C_p°$ value. Both a positive $\Delta S°$ and negative $\Delta C_p°$ for folding at 298 K are clear signatures of the hydrophobic effect playing a dominant role in structure stabilization in water.[17] This is also consistent with the high resistance to denaturation by urea exhibited by the hairpin as described above, with $\Delta\delta_{H\alpha}$ values in 7 M urea at 298 K being 62% of the values in aqueous solution at the same temperature. It is generally considered that urea disrupts intramolecular interactions by competing for hydrogen-bonding sites; it is perhaps not surprising, therefore, that urea has a relatively small effect on hairpin stability if folding is driven by the hydrophobic effect and not by hydrogen bonding, as implied by these data.

We have modeled the surface area buried on folding to rationalize the experimentally determined value for $\Delta C_p°$. The change in hydrophobic surface area (ΔA_{np}) on folding has been estimated by two methods, using a spherical probe of radius 1.4 Å. First, a value of between 450 and 600 Å^2 is obtained by measuring the change in hydrophobic area between the folded peptide (structure as determined below) and the peptide in various extended conformations representing a random coil. Secondly, we have summed the hydrophobic surface area of each of the 16 residues of the hairpin using Gly-X-Gly tripeptides as a model of the random coil state. This method gives a total surface area buried on folding of around 800 Å^2. For small molecules and proteins, the ratio $\Delta C_p°/\Delta A_{np}$ has typically been estimated in the range 1.4−1.75,[58] giving a calculated value for $\Delta C_p°$ for folding of the hairpin of between 700 and 1400 J K^{-1} mol^{-1}; the value determined experimentally is close to the upper limit of this range.

The role of organic solvents in promoting secondary structure formation is widely attributed to the promotion of intramolecular hydrogen bonding due to weaker competing solvent−solute interactions.[59−62] To gain insight into the thermodynamic basis for this increased stability, we have also investigated the thermodynamics of folding of the peptide in 20% (v/v) and 50% (v/v) methanol (Table 3). Notably, as the concentration of methanol increases, the change in heat capacity for folding decreases, becoming essentially zero for peptide folding in 50% methanol. This conclusion is consistent with calorimetric studies of the thermal unfolding of native ubiquitin and solubility studies of model compounds, where $\Delta C_p°$ is also shown to reduce to zero in >30% aqueous methanol.[63] The hairpin folding process becomes increasingly enthalpy-driven at higher concentrations of methanol, suggesting that hydrogen-bonding (electrostatic) interactions assume an important structure stabilizing role as the solvent environment changes. The observation in 20% methanol of protection from solvent exchange of NHs involved in interstrand hydrogen bonding supports this conclusion, while residues (spaced $i,i+2$) whose NHs face into solution show no such protection (unpublished results). The unfavorable conformational entropy term (that presumably largely accounts for the experimental $\Delta S°$ term for folding in mixed solvents, but which is masked by the entropic hydrophobic contribution to folding in water) becomes increasingly more negative as the folding process becomes more exothermic. Thus, better electrostatic (bonding) interactions are compensated by a more adverse conformational entropy term[64] as the peptide backbone becomes more constrained.

Conformation of an Isolated β-Strand (Residues 9−16). It is recognized that short-range interactions between two side chains or between a side chain and the adjacent peptide main chain are important factors in determining intrinsic conformational preferences[49] but can also lead to "non-random" behavior or local cooperative effects in denatured states of proteins and even short peptides. Hydrophobic clusters of residues have been identified in urea denatured proteins[65] or involving aromatic residues that stabilize β-conformations in small protein fragments.[44,66,67]

The role of these local interactions in predisposing the peptide to adopt the folded β-hairpin conformation described in this work, as well as providing a reference state against which the hairpin stability can be estimated (as described above), has been examined for a peptide fragment corresponding to the C-terminal β-strand of the hairpin (residues 9−16). The 8-mer is highly soluble in water and found to be monomeric, showing no concentration dependence of chemical shifts or line widths up

(58) Doig, A. J.; Williams, D. H. *J. Mol. Biol.* **1991**, *217*, 389.
(59) Nelson, J. W.; Kallenbach, N. R. *Biophys. J.* **1987**, *51*, 555.
(60) Arakawa, T.; Goddette, D. *Arch. Biochem. Biophys.* **1985**, *240*, 21.
(61) Storrs, R. W.; Truckses, D.; Wemmer, D. E. *Biopolymers* **1992**, *32*, 1695.
(62) Sonnichsen, F. D.; Van Eyk, J. E.; Hodges, R. S.; Sykes, B. D. *Biochemistry* **1992**, *31*, 8790.
(63) Woolfson, D. N.; Cooper, A.; Harding, M. M.; Williams, D. H.; Evans, P. A. *J. Mol. Biol.* **1993**, *229*, 502.
(64) Searle, M. S.; Westwell, M. S.; Williams, D. H. *J. Chem. Soc. Perkin Trans. 2* **1995**, 141.
(65) Neri, D.; Billeter, M.; Wider, G.; Wuthrich, K. *Science* **1992**, *257*, 1559.
(66) Lumb, K. J.; Kim, P. S. *J. Mol. Biol.* **1994**, *236*, 412.
(67) Dyson, H. J.; Sayre, J. R.; Merutka, G.; Shin, H.-C.; Lerner, R. A.; Wright, P. E. *J. Mol. Biol.* **1992**, *226*, 819.

to 8 mM. $^3J_{\alpha N}$ values, chemical shifts, and NOE intensity ratios have been determined to identify any intrinsic predisposition to adopt an extended β-strand conformation in the absence of the secondary structure interactions found in the hairpin.

While chemical shifts of H_α protons in the isolated C-terminal 8-mer showed very small deviations from random coil values (Figure 5c), in contrast, short-range NOEs and coupling constants deviate significantly from those expected in the random coil. Figure 4 shows the deviation of $^3J_{\alpha N}$ coupling constants from random coil values for the 8-mer for comparison with the hairpin under the same conditions. These values have been determined accurately ($\pm$0.2 Hz) for the 8-mer on account of the narrow line widths. The data reflect ϕ angle backbone conformational preferences; further, these deviations from random coil values are most pronounced at 303 K (data not shown), reflecting the temperature-dependent stability of the hairpin. Remarkably, $\Delta J_{\alpha N}$ values for the corresponding residues of the hairpin are quite similar to those for the shorter peptide (see Figure 4), indicating that, in many cases, the ϕ populations found in the partially folded hairpin in water are already present for the 8-mer. Many $^3J_{\alpha N}$ values for the 8-mer deviate from random coil values by $\geq$0.5 Hz and by up to 1.0 Hz in the case of Ser 15 (excluding the terminal Ile). To substantiate further these observations, we have determined the ratios of NOE intensities described above in section (ii). As is evident for the corresponding residues of the hairpin, NN(i,i+1) NOEs are either very weak or not detected. We estimate an αN(i,i+1)/NN(i,i+1) NOE ratio of at least 15 for all residues of the 8-mer, which strongly suggests a high proportion of β-(i)β(i+1) conformers. A quantitative estimate of the αN(i,i+1)/αN(i,i) ratio of NOE intensities gives values in the range 3.5−9 with the values at the higher end of the range significantly larger than the ratio ($\approx$2.3) predicted for a random coil. Thus, it is evident that the 8-mer is highly predisposed toward adopting the extended β-strand conformation found in the folded hairpin, presumably on the grounds of steric interactions between nearest neighbor β-branched residues and hydrophobic interactions that seem likely to stabilize this extended conformation. The observation that deviations from random coil values are most pronounced at 303 K is consistent with stabilization of an extended conformation by hydrophobic interactions between side chains spaced i,i+2 along the chain.

These data lead us to conclude that the changes in H_α chemical shift observed for the hairpin are largely a result of interstrand interactions. This conclusion is borne out by a closer analysis of $\Delta\delta_{H\alpha}$ values shown in Figure 5a,b. These display a pronounced i,i+2 periodicity such that inward-facing H_α protons directly opposed to the other strand in the folded structure show the largest shift changes. This conclusion is contrary to the generally held view that changes in H_α chemical shift largely reflect changes in the backbone torsion angle ϕ,[16,68] although the effects of interstrand interactions have been predicted from theoretical considerations.[69] The comparison between these parameters for the partially folded hairpin in water and the isolated β-strand has enabled us to dissect out the different contributions to the observed $\Delta\delta_{H\alpha}$ values in the hairpin. These appear to reflect largely formation of secondary structure rather than any local ϕ,ψ conformational preferences in the random coil or any dependency of H_α shift on ϕ.

These observations further support our use of Hα shift values to derive thermodynamic parameters: clearly, changes in Hα chemical shift only occur on hairpin formation and thus make an excellent probe of hairpin population. They also suggest that the unfolded state of the peptide is not a random structure but has strands already predisposed toward adopting an extended conformation. This may also partly explain why folding approximates so well to a two-state model.

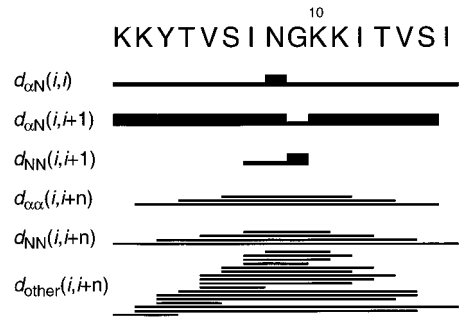

Figure 8. Summary of the NOE data for the β-hairpin in 20% (v/v) aqueous methanol at 278 K. Relative cross-peak intensities were estimated from volume integration and used subsequently in structure calculations. NOEs indicated as "other" interactions include long-range side chain−side chain and side chain−main chain interactions.

The use of coupling constant data for the estimation of folded conformers has been widely adopted. However, the coupling constants for the 8-mer in this study illustrate that $^3J_{\alpha N}$ values reflect a local structural parameter and that care should be taken in extrapolating this to an overall folded population. Although we may wish to conclude that a certain $\Delta J_{\alpha N}$ value reflects a certain population of hairpin secondary structure, the observation of similar $\Delta J_{\alpha N}$ values for the isolated β-strand and the corresponding residues of the hairpin in water emphasizes that $\Delta J_{\alpha N}$ values reflect local conformational preference and are not, in this context, a reliable measure of secondary structure formation.

Structure of the β-Hairpin in Solution. The large number of short- and long-range NOEs observed for the hairpin has allowed us to probe its structure in more detail. An ensemble of structures compatible with the experimental restraints have been calculated to identify the general features of the folded conformation. We have chosen to analyze the data under conditions in which there is a high proportion of folded structure present ($\approx$70%), namely in 20% methanol solution. The observation of a significant number of long-range main chain NOEs involving Hα and NHs (summarized in Figure 8), together with the conclusions from the thermodynamic data and NH protection pattern, is consistent with secondary structure stabilization by a network of hydrogen-bonding interactions between the two β-strands. A total of 170 NOEs were assigned and quantitated for use in structure calculations (see methods) with pseudo atom corrections applied where necessary using the distance modify command of DYANA.[27] The NOEs were broken down into 86, 51, 14, and 19 intraresidue, short-, medium-, and long-range restraints, respectively. A total of 30 torsional angle restraints for ϕ and ψ were determined by a combination of short-range HN−Hα NOEs and the $^3J_{\alpha N}$ coupling constants using HABAS. Restraints were checked for impact on structure by the distance check function which reported good scores for all the long-range restraints, indicating that there were no "lonely" NOEs which would have a high impact on the structure.

Initially, 30 structures were generated randomly. The 200 constraints (170 distance and 30 angle) were applied to the system and simulated annealing was performed using torsion angle dynamics employing the standard "anneal" macro of DYANA (see Materials and Methods). The 30 annealed

(68) Serrano, L. *J. Mol. Biol.* **1995**, *254*, 322.
(69) Osapay, K.; Case, D. A. *J. Biomol. NMR* **1994**, *4*, 215.

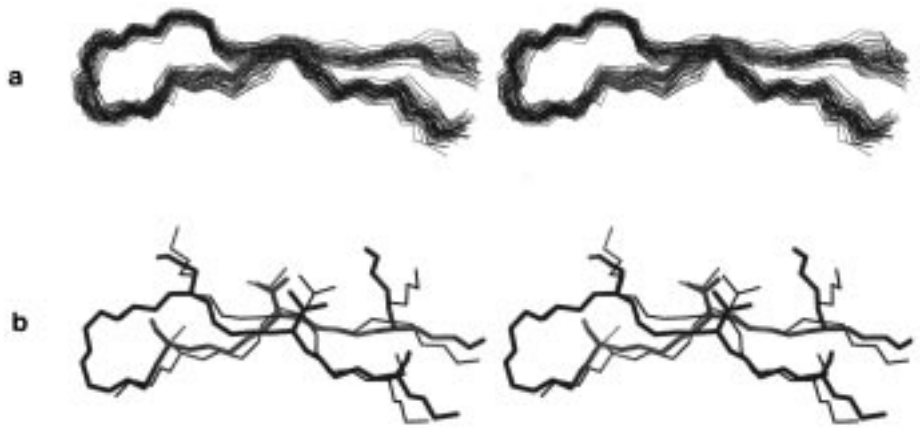

Figure 9. (a) Stereoview of 60 overlayed structures (backbone only) of the β-hairpin representing 10 snapshots from each of six dynamics runs at 300 K (see text). The RMSD to the mean structure is 0.6 ± 0.2 Å. (b) Stereoview of the mean structure superimposed on the two β-strands of the *met* repressor dimer (thin lines). The residue side chains (K2, T4, S6, K11, T13, and S15; hairpin numbering) on each strand that are involved in DNA recognition are also illustrated.

structures were sorted according to quality, as measured by the DYANA target function. The whole range of structures was hairpin shaped, with a moderate pairwise RMSD from the backbone of the mean structure (2.1 ± 0.6 Å). Analysis by the WHATCHECK algorithm[30] of the middle 14 residues, and excluding glycine, reveals that 89% are in allowed regions of Ramachandran space, showing the structures to be of moderate quality.

Three of the structures (the best, second best, and tenth best) were then used as starting structures for molecular dynamics using the SANDER module of AMBER 4.1.[28] Each of the three starting structures were minimized and then subjected to two 100-ps restrained molecular dynamics runs, each with a different random number seed in the initial velocity assignments, to give six final structures. The set of restraints previously described were used, with two additional restraints to the acetyl methyl group. The low-temperature structures from the simulated annealing protocol had a backbone RMSD from the mean structure of 0.5 ± 0.1 Å, which increases to 1.0 ± 0.2 Å when all heavy atoms are considered. WHATCHECK analysis revealed that none of the residues were in disallowed regions of the Ramachandran plot. The structures had an average distance restraint deviation of 0.05 ± 0.01 Å and an average angle restraint deviation of 2 ± 2°. Furthermore, there appeared to be no correlation between starting structure and final structure, suggesting that the results are not unduly biased by the initial geometry of the DYANA starting structures.

An ensemble of 60 overlayed structures (backbone only) are shown in stereo in Figure 9a and represent 10 structures from each of the six separate dynamics runs collected between 70 and 80 ps of the 100-ps run at 300 K. The RMSD from the mean of the 60 structures was 0.6 ± 0.2 Å. The two strands of antiparallel β-sheet are connected by a type I′ turn, with Asn 8 occupying the left-handed (α_L) region of conformational space (Figure 10a). Noticeably, the hairpin has the characteristic right-handed twist exhibited by most protein β-sheets[39,41] and as required for DNA major groove recognition,[31] as illustrated in Figure 9b. A combination of experimental restraints and the AMBER 94 force field seems to reproduce this structural feature rather well. The coordinates of the 60 overlayed structures shown in Figure 9a are available from the authors on request, together with a full listing of NOE and torsion angle restraints used in structure calculations.

Comparison of the β-Hairpin Structure with the Two Strands of the DNA Recognition Motif of the *met* Repressor Dimer. The backbone ϕ and ψ torsion angles of 60 structures (Figure 9a), sampled at 300 K over 10 ps of each of the six molecular dynamics runs, are shown in the Ramachandran plot of Figure 10a. It is evident that most of the residues are located in the β-region, with the residues Gly (marked by a cross) and Asn lying in the left-handed α_L region, characteristic of a type I′ turn. The spread of backbone angles for each residue in the ensemble of structures is shown in Figure 10b. Also included are ϕ and ψ values (larger dots) for the two anti-parallel strands of β-sheet from the crystal structure of the *met* repressor−DNA complex.[31] A superposition of backbone atoms of the residues of the two strands on to those of the 60 β-hairpin structures gives a pairwise RMSD of 1.0 ± 0.2 Å. The interstrand hydrogen-bonding pattern of the hairpin is identical to that of the dimer, such that side chains on one face of the hairpin are presented in an orientation appropriate for binding to DNA. The RMSD between backbone atoms and side chains of the six residues on the DNA recogition face (K2, T4, S6, K11, T13, and S15), calculated in the same way as described above, was found to be higher (1.6 ± 0.2 Å); however, this included the flexible side chains of the lysines which are likely to show a much greater degree of disorder in the free peptide than when restrained upon binding to DNA. The similarity in backbone conformation and orientation of residues side chains involved in binding is evident from the overlay of the mean of the 60 structures with the two strands of the *met* repressor β-sheet shown in Figure 9b. A combination of the right-handed twisted conformation of the hairpin and its pattern of interstrand hydrogen bonding and side chain orientations suggest that the hairpin conformation may be predisposed to DNA recognition and binding. DNA binding studies are currently in progress and will be reported in due course.

Conclusions. The origin of the stability of autonomously folding β-hairpins in aqueous solution has been far from clear, with contrasting opinions as to the relative importance of the different factors, including interstrand hydrogen bonding,[9] hydrophobic interactions,[7,8] and conformational preference (steric factors) relating to the turn sequence.[5,11] In this work we have shown that the folding of a model β-hairpin peptide approximates well to a two-state transition and have described a detailed structural and thermodynamic characterization that shows that the peptide folds in water with the temperature-

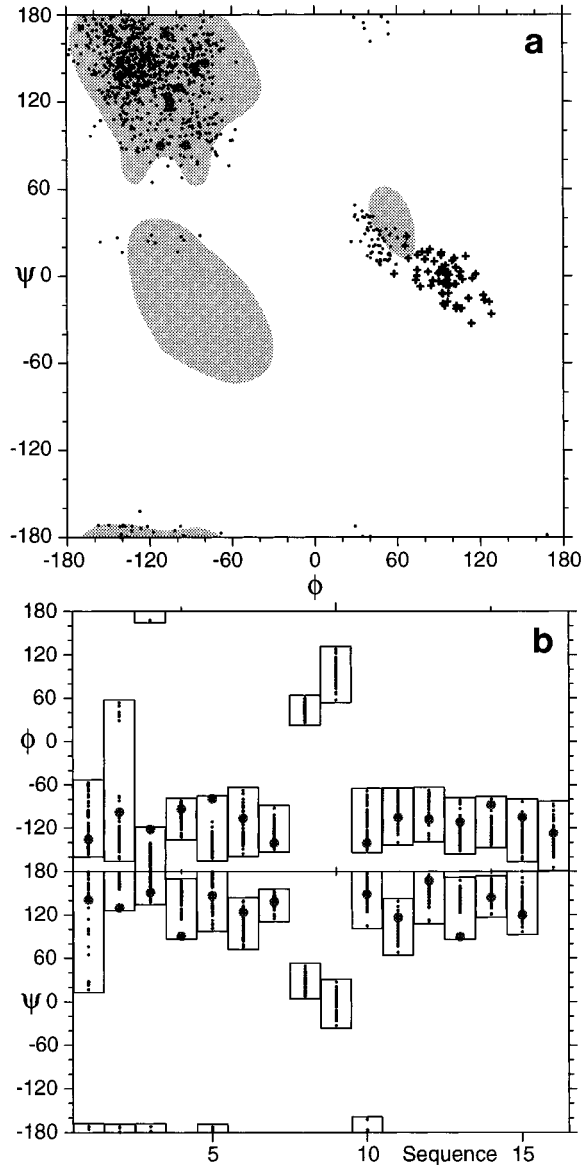

Figure 10. (a) Ramachandran plot of backbone ϕ,ψ angles for the 60 overlayed structures shown in Figure 9a. Gly ϕ,ψ angles are marked by a cross; together with those of Asn, these residues lie in the α_L region characteristic of a type I′ turn. Larger dots represent the ϕ,ψ dihedral angles of the two strands of the *met* repressor dimer which also lie in favoured β-space. (b) ϕ,ψ distribution plot showing the range of ϕ and ψ values adopted by each residue amongst the ensemble of 60 structures. Again larger dots represent the ϕ,ψ values for the two β-strands of the *met* repressor dimer. Figures were generated using MOLMOL.[29]

dependent characteristics reminiscent of proteins with hydrophobic cores.[17] Folding in water is endothermic and is associated with a large negative $\Delta C_p°$ establishing, at least for this model system, that the hydrophobic effect plays a major structure-stabilizing role in water. The population of folded hairpin structure has been estimated by three independent methods, namely temperature dependence of Hα chemical shifts, CD using the ellipticity value at 216 nm, and the intensity of interstrand Hα−Hα NOEs; all three methods are in general agreement.

We have investigated the nature of the unfolded state of the hairpin by characterizing a peptide fragment (residues 9−16) corresponding to the C-terminal β-strand of the hairpin. $^3J_{\alpha N}$ values and the intensity of backbone NOEs between nearest neighbor residues are not consistent with a random coil conformation but indicate that the peptide has a natural propensity to adopt an extended β-strand conformation, showing it to be predisposed to forming β-hairpin secondary structure. In contrast, Hα chemical shifts for this short peptide are close to random coil values and are not found to be sensitive to the local conformational preferences identified from coupling constants. These data strongly suggest that deviations of Hα shifts from random coil values largely reflect the anisotropic effects arising from interstrand interactions, that is secondary structure formation, in agreement with the conclusions of Osapay and Case.[69] These results emphasize the importance of accurately determining reference states for the purpose of estimating populations of folded conformers. While the three methods described above (NOEs, CD, and Hα shifts) assess interstrand interactions, $^3J_{\alpha N}$ values need to be treated with some caution in sequences that are rich in β-branched residues because of local cooperative interactions that affect backbone conformational preferences.

The recent studies highlighted in the introduction have demonstrated the important role of turn sequences in dictating the register of hydrogen-bonding interactions in the flanking strands. Clearly, residue-specific conformational preferences do play an important role,[5,11] but does the turn sequence exert a stabilizing effect on the β-hairpin conformation or simply exclude certain conformations or alternative folding arrangements on steric and entropic grounds? In the present study, we chose the Asn-Gly sequence due to its high frequency in type I′ turns in the Protein Data Bank. Some insight into why this should be such a favorable turn sequence comes from an analysis of conformational preferences in the random coil using data derived from the coil regions of high-resolution crystal structures.[49,50] The statistical analysis reveals that Asn and Gly are the only amino acids which have a significant population of the left-handed region (α_L) of ϕ,ψ space required for the type I′ turn. However, these residues only populate this region of conformational space to a small extent compared with the core regions of α and β space (Asn: α_L < 20%, cf. $\alpha + \beta \approx$ 80%). Thus, while this data provides a rationale for the formation of a type I′ turn at the Asn-Gly sequence, it also suggests folding will not be driven by the conformational preferences of the turn residues alone, since they prefer to be in α or β conformation. It is more that these preferences must be compatible with the folded structure which, in this case, appears to be stabilized in water by hydrophobic interactions between the side chains of the two opposing β-strands. It would seem that the Asn-Gly sequence is better described as "not bad" rather than a "good" turn.

Acknowledgment. We acknowledge the support of the EPSRC (Studentship to A.J.M.), the BBSRC (G.J.S.), The Royal Society, Nuffield Foundation, and the Department of Chemistry at the University of Nottingham for financial support. We thank John Keyte in the School of Biomedical Sciences, University of Nottingham, for solid-phase peptide synthesis and for allowing us access to HPLC facilities.

Supporting Information Available: Table of NOE and torsion angle restraints for structural calculations (2 pages). See any current masthead page for ordering and Web access instructions.

JA9726769